

First order optoelectronic correlation utilizing metal-semiconductor-metal photodetectors

Syoji Yamada, Tsuneo Urisu, Takayuki Sugeta, and Yoshihiko Mizushima
Electrical Communication Laboratories, Nippon Telegraph and Telephone Public Corporation 3-9-11,
Midoricho, Musashino-shi, Tokyo, 180 Japan

(Received 9 November 1982; accepted for publication 4 January 1983)

Optoelectronic correlations between two *n*-GaAs metal-semiconductor-metal photodetectors were measured. An arrangement of two photosensing areas, each having a separation of far less than the minimum possible wavelength on the stripline, was examined. The equivalent circuit analysis clearly explained the observed correlation signals and revealed the limits of the photodetector response.

PACS numbers: 41.70. + t

Recently, various types of picosecond photodetectors having a metal-semiconductor-metal (MSM) stripline structure have been demonstrated. Their operation mechanisms are divided into two groups; one is transit time (between electrodes) limited,^{1,2} and the other is (carrier recombination) lifetime limited.^{3,4} Although the latter has an ultrafast response,⁴ it has the demerit of low sensitivity. For the former, one or two orders of magnitude higher sensitivity is expected.

To measure the response of fast photodetectors, an optoelectronic linear correlation method^{5,6} has recently been proposed. Although it has the advantage of being simple and more sensitive in comparison with nonlinear optical correlations, such as second harmonic generation, the output signal depends on the transient behavior of the detector, device parameters, and circuits. For these applications, therefore, it is important to clarify the correlation mechanisms.

In the present work, optoelectronic correlations between two MSM photodetectors¹ were measured using a picosecond light pulse source. Relations between the incident optical pulse waveform and the correlation signal via the response of the photodetectors were formulated and equivalent circuits for the correlation were obtained. The calculation was found to explain clearly the measured signals, and estimate the response limit of the photodetector.

Details of the MSM photodetector structure were described in a previous paper.¹ The material is a nondoped *n*-type GaAs ($n \approx 10^{15}/\text{cm}^3$) epitaxial layer having a thickness less than $6 \mu\text{m}$. The real time response had a 60-ps rise time and a 90-ps full width at half-maximum (FWHM). The light pulse source of less than a 10-ps duration was a mode-locked Oxazine 725 dye laser. The incident energy per pulse at 700 nm was estimated to be about 30 pJ.

Here, the following two types of correlation experiments were carried out.

Type (A). As examined in Ref. 4, two photodetectors (PD1, PD2) were connected in series via a coaxial cable with a 3-dB attenuator inserted between them. Two split light pulse beams irradiated each of the sensing area. Only one photodetector PD1 was dc biased. Therefore, PD2 becomes operative only when the PD1 output signal pulse arrives in it, and the correlation signal, that is, the time averaged output from PD2 was measured as a function of the delay time τ_d between the two incident light pulses.

Type (B). As a new arrangement, two photosensing areas (S1, S2) were very closely fabricated on one chip, as shown in Fig. 1. This separation was far less than the minimum possible wavelength on the stripline. Therefore, the operations of the two sensing areas are mutually interactive. In this case, both sensing areas were biased. The method of correlation signal measurement was similar to that in type (A).

The observed correlation signals are shown in Figs. 2(a) and 2(b) with open circles for types (A) and (B), respectively. In the case of (A), the correlation signal is, as expected, composed of a fast rising part closely corresponding to the time integration of the PD1 output signal and a slowly falling tail determined almost entirely by the recombination lifetime of the material. In case (B), both sensing areas are biased and the correlation signal becomes narrower and includes a relatively large background. The ringing feature observed in this signal is, as will be discussed later, probably due to the inductance of the bonding wire which is attached to the middle of the center conductor.

In a one-dimensional (x) analysis of the semiconductor,

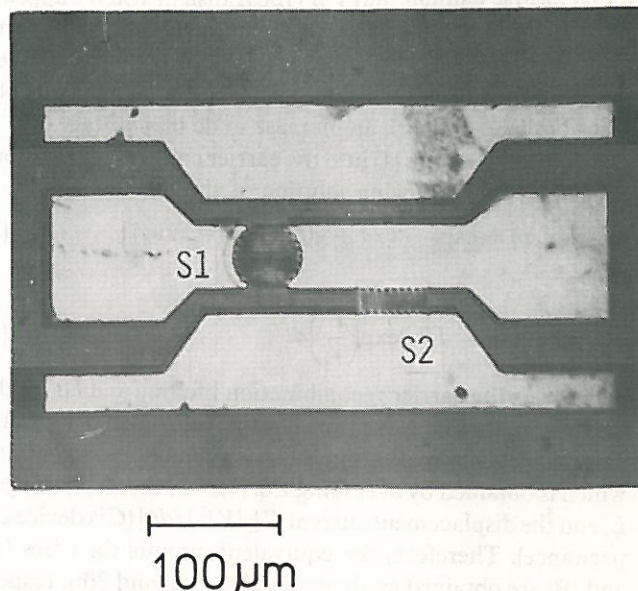


FIG. 1. Top view of the MSM photodetectors used in the type B correlation experiment. S1 and S2 are the photosensing regions made of interdigital electrodes.

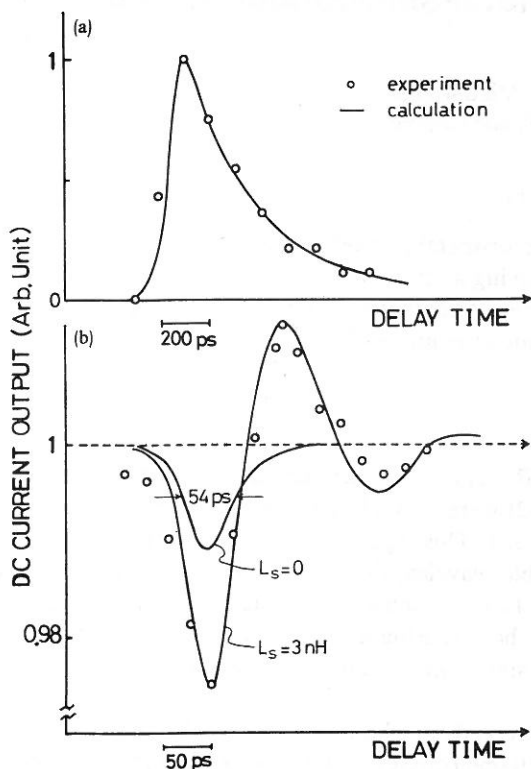


FIG. 2. Observed and calculated correlation signals. (a) is for type (A) and (b) for type (B) configuration. The comparison between experiments and calculations was carried out by peak normalizing for (a) and background normalizing for (b).

the transient photocurrent density $j_c(x, t)$ under dc bias is represented by

$$j_c(x, t)$$

$$\approx qn(x, t)v_n[1 + \alpha V(t)] + qp(x, t)v_p[1 + \alpha V(t)], \quad (1)$$

where q is the unit charge, $n(x, t)$ and $p(x, t)$ the photoexcited electron and hole densities, $V_{n(p)}$ the carrier drift velocity under dc bias voltage, and $V(t)$ the transient voltage appearing in the device. The velocity field characteristic of the form $v[1 + \alpha V(t)]$ having a small constant α was assumed, since the amplitude of the real time photocurrent signal was observed to increase with an increase in dc bias voltage.

Substituting Eq. (1) into the carrier continuity equation, one obtains the following solution of $n(x, t)$:

$$n(x, t) = \exp(-t/\tau_1)[g(t) - g(t - x/v_n)] \quad (2)$$

and

$$g(t) = \int_{-\infty}^t l(t') \exp\left(\frac{t'}{\tau_1}\right) dt', \quad (3)$$

where τ_1 is the carrier recombination lifetime and $l(t)$ is the incident light pulse waveform. The total current of the photodetector is given by the sum of the conduction current $i(t)$, which is obtained by averaging Eq. (1) over the electrode gap L , and the displacement current $C[dV(t)/dt]$ (C is device capacitance). Therefore, the equivalent circuits for cases (A) and (B) are obtained as shown in Figs. 3(a) and 3(b), respectively.

In these figures, R_l and R_s are the matching resistance equal to 50Ω . The suffixes 1 and 2 indicate the quantities

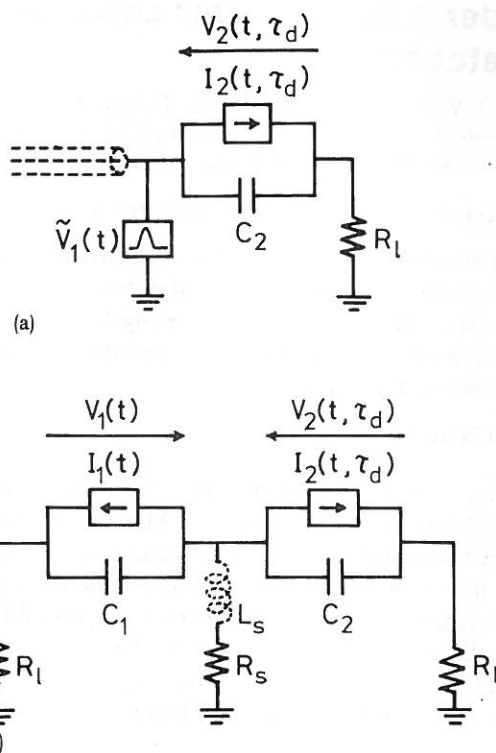


FIG. 3. Equivalent circuits for correlation signal calculations. (a) is for type (A) and (b) is for type (B) configuration.

related to PD1 and PD2, respectively. In Fig. 3(a), the transient voltage generated by PD1 is represented by the voltage source $\tilde{V}_1(t) = i_{t1}Z_0$, where i_{t1} is the total current of PD1 and Z_0 is the line impedance.

The dc correlation signal calculated for the present cases (A) and (B) are drawn with solid lines in Figs. 2(a) and 2(b), respectively. The drift velocities used were $v_n = 10^7$ cm/s and $v_p = 7.5 \times 10^6$ cm/s. The electrode gaps were $5 \mu\text{m}$ (case A) and $2 \mu\text{m}$ (case B), and the corresponding capacitance values were estimated to be 0.37 and 0.13 pF, respectively. A one-sided exponential function with a 10-ps FWHM was used for the incident light pulse waveform $l(t)$.

Comparing the calculated results with those of the experiments in Fig. 2(a), the effective carrier lifetime τ_1 for used n-GaAs has been found to be about 300 ps. In order to ex-

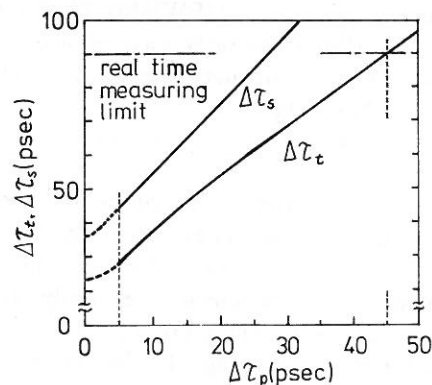


FIG. 4. Calculated dependence of FWHM of the correlation signal $\Delta\tau_c$ and the true detector response $\Delta\tau_s$ on the optical pulse FWHM $\Delta\tau_p$. Real time measurement is limited in the region $\Delta\tau_c \gtrsim 90$ ps.

plain the ringing feature in the signal in Fig. 2(b), a minor inductance $L_s = 3$ nH is assumed in the calculations in addition to R_s , as shown in Fig. 3(b). Good agreement between the calculated and observed signals is obtained as shown in Fig. 2(b). If $L_s = 0$, the calculation results show no ringing as can also be seen in the figure.

With this calculation, the pulse width (FWHM) of the correlation signal $\Delta\tau_s$ and the detector response $\Delta\tau_t$ when $L_s = 0$ are shown in Fig. 4 as a function of the incident light pulse width $\Delta\tau_p$ (FWHM) for type (B) correlation. Applying this figure to the observed correlation signals, $\Delta\tau_t$ and $\Delta\tau_p$ are roughly determined from the observed $\Delta\tau_s$.

The value of $\Delta\tau_s = 54$ ps gives $\Delta\tau_p = 10$ ps which is very close to the SHG autocorrelation measurement. It is noted that $\Delta\tau_s$ and $\Delta\tau_t$ are nearly saturated instead of falling to 0 in the $\Delta\tau_p \lesssim 5$ ps region in Fig. 4. This indicates that the photodetector response limit, determined by the transit time and the capacitance in the present case, is about $\Delta\tau_t = 30$ ps.

In other words, the measurement range which is limited to $\Delta\tau_p \gtrsim 45$ ps for $\Delta\tau_t \gtrsim 90$ ps in the real time detector pulse measurement has expanded by an order of magnitude down to $\Delta\tau_p \gtrsim 5$ ps by using the correlation method. Utilizing photodetector of shorter response limit, a few picosecond $\Delta\tau_p$ measurements can be realized with higher sensitivity than SHG technique. For this purpose, detectors with much smaller transit time must be fabricated.

¹T. Sugeta, T. Urisu, S. Sakata, and Y. Mizushima, *Jpn. J. Appl. Phys.* **19-1**, 459 (1979).

²J. Degani, R. F. Lehny, R. E. Nahory, M. A. Pollack, J. P. Heritage, and J. C. DeWinter, *Appl. Phys. Lett.* **38**, (1981).

³D. H. Auston, P. Lavallard, N. Sol, and D. Kaplan, *Appl. Phys. Lett.* **36**, 66 (1980).

⁴P. R. Smith, D. H. Auston, A. M. Johnson, and W. M. Augustyniak, *Appl. Phys. Lett.* **38**, 47 (1981).

⁵D. H. Auston, P. R. Smith, A. M. Johnson, and J. C. Bean, *Appl. Phys. Lett.* **37**, 371 (1980).

⁶D. H. Auston and P. R. Smith, *Laser Focus* **18**, 89 (1982).